

Short Communication

Surface Structure Sensitive Electrocatalytic Activity of Platinum Nanofilm Decorated Gold Microelectrode for Oxygen Reduction Reaction

Deyu Qu¹, Youzhen Tao¹, Liping Guo¹, Zhizhong Xie¹, Wena Tu² and Haolin Tang^{2,*}

¹Department of Chemistry, School of Chemistry, Chemical Engineering and Life Science, Wuhan University of Technology, Wuhan 430070, Hubei, P.R. China

²State Key Laboratory of Advanced Technology for Materials Synthesis and Processing, Wuhan University of Technology, Wuhan 430070, Hubei, P.R. China

*E-mail: thln@whut.edu.cn

Received: 18 December 2014 / Accepted: 17 January 2015 / Published: 24 February 2015

The electrocatalytic activity toward oxygen reduction reaction of a Pt nanofilm decorated gold microelectrode with various of Pt/Au surface ratio has been investigated. The surface ratio of Pt over Au on the electrode is precisely controlled through Cu under potential deposition followed by the surface limited redox replacement reaction with Pt complex ions. Microelectrodes are applied to study the oxygen reduction diffusion-limited current. It turns out that Pt-Au bimetallic catalyst toward oxygen reduction reaction exhibits a surface ratio dependent activity. The variation of reduction kinetic current density as well as the value of onset potential is observed with respect to the Pt/Au surface ratio. The highest specific activity and most efficient utilization of Pt for oxygen reduction reaction is observed with the Pt/Au ratio of 0.62. The results demonstrate that microelectrode-based technology is a promising way to determine the electrocatalytic activity and also provide an idea to design low Pt content electrocatalysts for oxygen reduction reactions.

Keywords: fuel cell; oxygen reduction; electro-catalytic activity; microelectrode; surface ratio dependent

1. INTRODUCTION

Electrochemical energy storage systems have attracted increasing attentions recently due to the concerns related to depleting fossil fuels and global warming. Pt is currently used as the catalyst for the O₂ reduction reaction (ORR) in fuel cells. Besides the cost of Pt, it also suffers other limitations e.g. low tolerance of the poisonous species adsorption.[1-5] To alleviate those problems, catalyst with high

activity and durability is required. Pt-based bimetallic materials with hetero-structure have attracted particular attention in recent days.[3,4,6-24] For example, Pt-Pd bimetallic nano-dendrites were found to have higher electro-catalytic activity toward ORR than that of Pt alone.[15] The enhancement of catalytic activity toward ORR for the Pt-based bimetallic catalysts was believed to be resulted from the modification of surface structure, change of d-band vacancy and therefore affecting the binding energy of O₂ and the activation energy of OH formation.[11,21,22,25] Among various Pt-based bimetallic catalysts, Pt-Au and its electro-catalytic activity toward ORR and methanol oxidation have been widely investigated.[3,4,6,7,9-14,16-20,26-29] Previous studies indicated that the Pt-Au electrode exhibited excellent catalytic activity to ORR. With the presence of Au, the stability and durability of Pt-based catalyst increased particularly due to the suppression of Pt dissolution and migration in the course of ORR.[3,16-18,20] More importantly, through the modification of the electronic band structure and the surface energy, Pt-Au bimetallic material reveals an improved catalytic activity and then make ORR more efficient.[6,7,21] Recently, the Pt-Au catalyst was also used in Li-air battery. This bi-functional catalyst showed high activity toward oxygen evolution reaction as well as oxygen reduction reaction.[23,24] Since the Pt-Au bimetallic catalyst demonstrates the potential for the enhancement of catalytic activity toward ORR, it is necessary to optimize the composition of such catalyst. Most of the optimization research, however, focused on the ratio of Pt to Au mass loading.[7,10-12] Apparently, instead of the mass ratio, it is the ratio of the surface composition and structure that are critical for the Pt-Au electro-catalytic activity on ORR. In the present study, the surface composition of Pt-Au was precisely controlled through the formation of coverage-controlled under potential deposition(UPD) of Cu adlayer and followed by the surface limited redox replacement reaction with different Pt complex ions.[10,14,30-32] The catalytic activity of a Pt/Au electrode for ORR with various Pt/Au surface ratios was systematically investigated. It was observed that the Pt/Au surface ratio of 0.62 exhibited the highest activity for ORR.

2. EXPERIMENTAL DETAILS

CuSO₄•5H₂O (99.999%), K₂PtCl₄ (99.9+%) and K₂PtCl₆ (99.9+%) were purchased from Aldrich. H₂SO₄ (suprapure grade) and HClO₄ (suprapure grade) are obtained from Wako Pure Chemicals. They were used as received. Water was purified using a Milli-Q purification system (Millipore).

A Au microelectrode was used for the kinetics study of ORR. There are several advantages by using microelectrode over its large counterpart, such as the significant increased mass transport rates to and from the microelectrode, reduced double-layer capacitance and neglected IR drop. Therefore, when the size of the electrode reduced to a certain value causing a reduction of transient diffusion response, a steady state of mass transport can be established. The mass transport to and from a microelectrode can be equivalent to that of a rotation disk electrode (RDE). The mass transport on a microelectrode with a smaller diameter is equivalent to that on a RDE with a higher rotation rate.[33] Previous study showed that the limiting current for oxygen reduction can be achieved in the microelectrode.[33] The Au microelectrode was prepared as before.[33] The surface area of the Au

microelectrode was estimated from the cathodic current corresponding to the reduction of Au oxide to be 0.14 mm^2 , which is similar to that in the previous study. [33,34,35]

The electrochemical measurements were conducted using a CH Instruments 660C electrochemical workstation equipped with a CHI 201 Picoamp Booster for microelectrode measurements. A SCE electrode was used as reference electrode. Scan tunneling microscope (STM) measurements were carried out by using a NanoScope E (Digital Instrument) with a homemade electrochemical STM cell. STM images were obtained in constant current mode. STM tips were prepared from Pt-Ir (8:2) wire (Tanaka Precious Metal) by mechanical cutting. STM observations were carried out on an atomically flat (111) facet formed on the surface of a gold single-crystal bead which was prepared by Clavilier method.[36]

The Pt/Au electrodes were thoroughly cleaned with a freshly made 0.5 M sulfuric acid solution before the measurements of cyclic voltammogram (CV) and linear scan voltammetry (LSV) were conducted. Electrochemical active surface area (ECSA) of a Pt nanofilm was estimated from the amount of charge associated with the hydrogen adsorption/desorption[37]. The charge density of $210 \mu\text{C}/\text{cm}^2$, which is equivalent to the electrochemical adsorption/desorption of one hydrogen full monolayer on a polycrystalline Pt surface, was used.[32,34] The surface area of the Au microelectrode was estimated from the cathodic current corresponding to the reduction of Au oxide, the detailed procedures were described in ref.38.

3. RESULTS AND DISCUSSION

After thoroughly cleaned, the Au microelectrode used as the substrate for the formation of Pt nano-film was first characterized by cyclic voltammetry (CV). The readiness of the Au surface was revealed with the cyclic voltammogram of a clean polycrystalline Au electrode. The formation of Pt nano-film on Au electrode with different Pt-Au surface ratio was reported before.[10,30-32] A Cu mono/submono layer was formed on Au surface through UPD. The surface coverage of Cu adlayer was controlled by the applied UPD potential. As shown in Figure 1, different amount of Cu was deposited on the Au micro-electrode by holding the electrode at different UPD potentials. The Cu adlayer was then stoichiometrically replaced with Pt by the galvanic exchange with PtCl_4^{2-} or PtCl_6^{2-} complex ions through surface limited redox replacement reaction. The STM image, which provides the structure of the Pt-nanofilm on Au substrate, is shown in Figure 2. The Pt cluster associating with uncovered Au (111) surface is observed. It clearly shows that, after redox replacement, the Pt does not homogeneously deposit on Au substrate, surface aggregation of the Pt ad-atoms takes place. This surface aggregation causes the formed Pt film having two monolayers, about 0.4 nm height which is clearly shown in the cross section analysis at Figure 2B. Since this surface aggregation process is believed to be time-dependent,[30, 32] the Au micro-electrode with different coverage of Cu ad-layer have been incubated in Pt complex ions solution for 4 hours in this study.

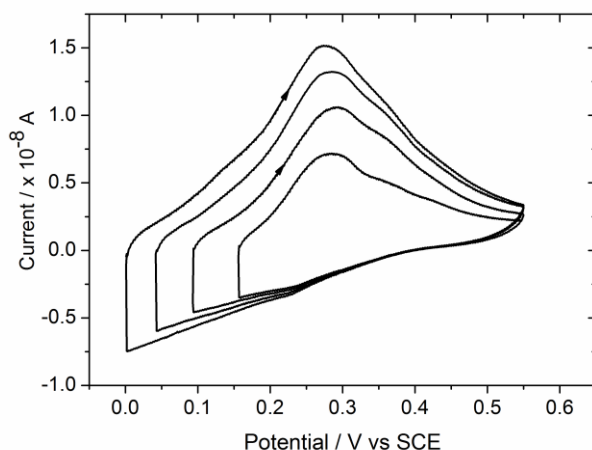


Figure 1. Cyclic voltammograms of UPD Cu on Au microelectrode in 0.05 M H₂SO₄+ 5 mM CuSO₄ solution with potential scan rate of 50 mV s⁻¹

It must be noted here that the STM image was taken on an atomically flat Au(111) facet not the micro-electrode which was used in electrochemical measurements. The resulted microelectrode was then tested by CV measurements in 0.05 M H₂SO₄ solution. The result was shown in Figure 3. The gold oxide reduction peak around 0.85V, the platinum oxide reduction peak around 0.4 V as well as a well-shaped hydrogen adsorption/desorption features in the potential region of + 0.1V to - 0.20 V were all observed, indicating the formation of a Pt/Au bimetallic surface.

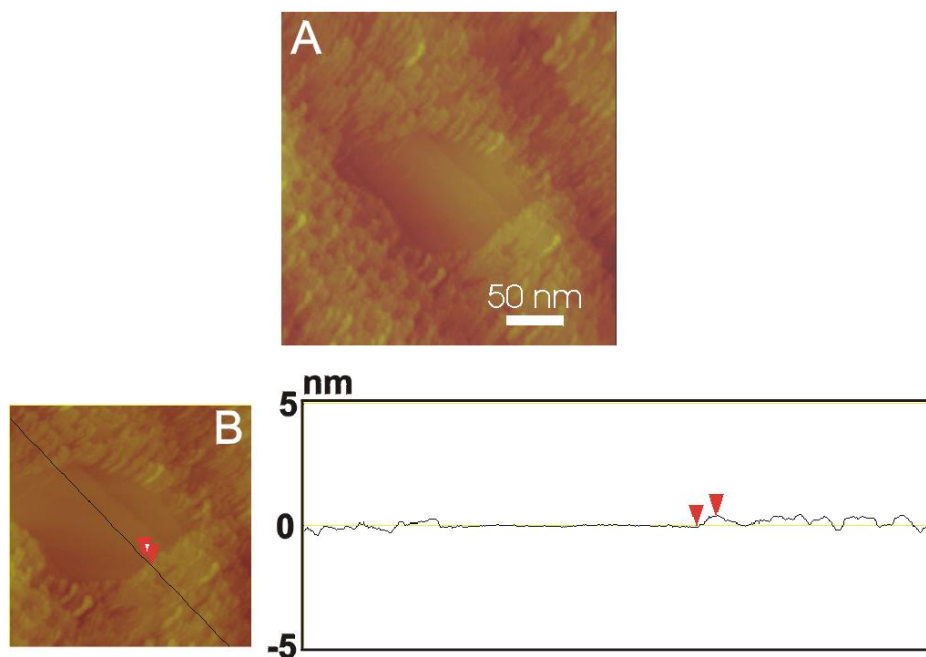


Figure 2. STM images ($U_t = 100$ mV, $I_t = 100$ pA) of Pt nano-film on Au (111) electrode obtained after 4 hours replacement of Cu adlayer formed on Au (111) electrode surface with applied UPD potential of 0 V with PtCl₄²⁻ complex ions. The electrode was rinsed by Pt ions free acidic solution before the STM image taken.

Before each ORR investigation, the stability of Pt-Au microelectrode was examined by CV in 0.05 H₂SO₄ solution. About 50 cycles of voltammograms were recorded and there are no changes observed, this indicated a high stability of the studied Pt-Au microelectrode. The ECSA of Pt-Au microelectrodes with different surface ratio were found all close to 0.14 mm². This ensured the steady state respond of microelectrode for all the surface components. The solid and dash line in Figure 3 represent the 2nd and 50th cycle of Pt/Au bimetallic electrode, respectively. It clearly shows that both CVs are almost identical indicating the stabilized surface structure of Pt nano-film on Au microelectrode. The Pt-Au bimetallic microelectrodes with seven surface ratios of Pt/Au were used in this study. The Pt/Au surface ratio was calculated from the ECSA of Pt nano-film divided with uncovered surface area of Au[39].

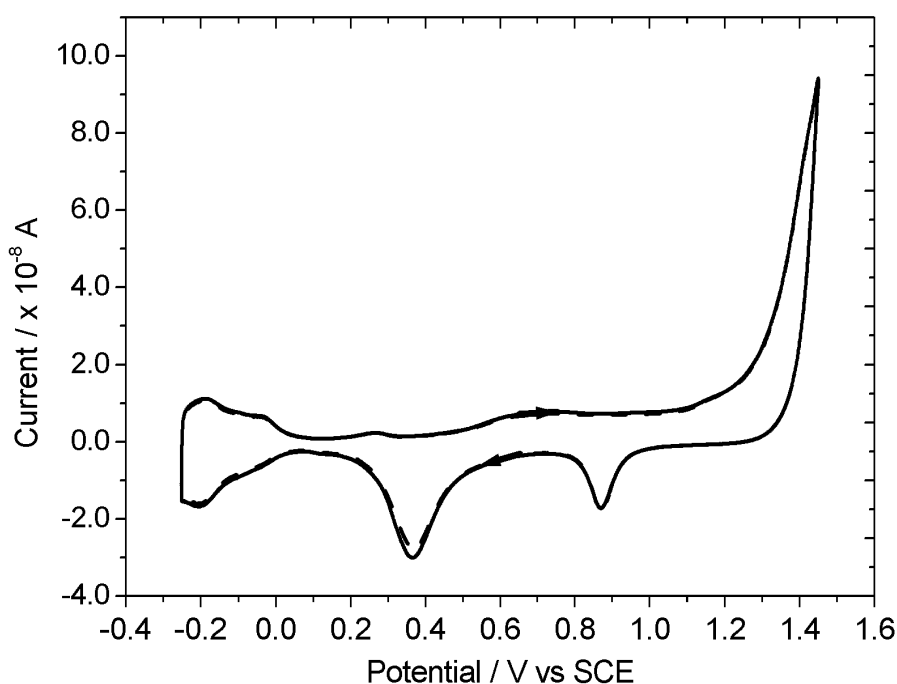


Figure 3. Cyclic voltammograms of Pt-Au microelectrode in 0.05 M H₂SO₄ solution with potential scan rate of 50 mV s⁻¹. Pt/Au surface ratio is around 2.0.

The electro-catalytic activity of the Pt-Au bimetallic microelectrodes with different Pt-Au surface ratios are investigated for ORR in an O₂-saturated 0.1 M HClO₄ solution. The profiles of LSV are shown in Figure 4. The ORR curves in Figure 4 represent the average of these three sets of data. In order to better compare the efficiency of the different Pt-Au electrodes, the current were normalized to the ECSA of Pt. Apparently, a kinetic-diffusion controlled region and a subsequent diffusion limited region could be distinguished, as labeled in inset graph in figure 4. The variation of reduction diffusion-limited current can be addressed to the different degrees of Pt dispersion on Au microelectrode. The ORR onset potential, P_{onset} and current density, I₀₂₅ (current density at the half-wave potential in the kinetic-diffusion control region of the ORR curve recorded with Pt bulk

electrode.) for the electrodes with various Pt-Au surface ratio were used to determine the electro-catalytic activity and tabulated in table 1.[6] The $I_{0.25}$ here was served as an indicator to compare the value of current density for ORR.

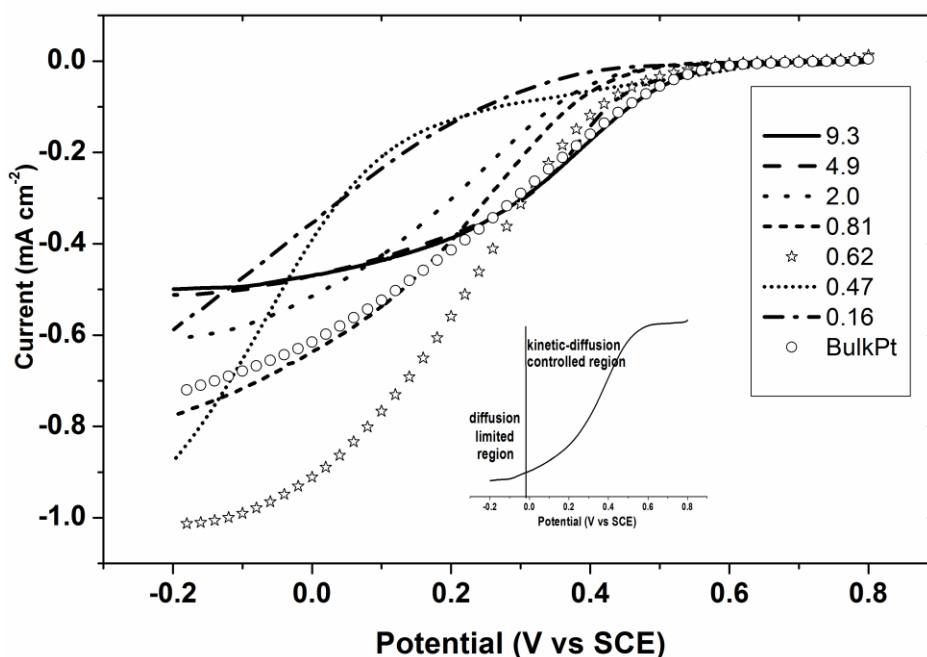


Figure 4. Linear scan voltammograms of Pt/Au microelectrode with different surface ratios in 0.1 M HClO₄ solution, saturated with O₂ at potential scan rate of 50 mV s⁻¹. LSV of polycrystalline Pt microelectrode is included in as a circle for comparison. Surface ratio of Pt/Au: 0.16 (dash dot), 0.47 (short dot), 0.62 (star), 0.81 (short dash), 2.0(dot), 4.9(dash) and 9.3 (solid).

Table 1. Comparison of onset potential, P_{onset} and kinetic current density, $I_{0.25}$ for ORR at Pt-Au bimetallic microelectrode with various surface ratios.

Pt/Au surface ratio	Onset Potential(V)	$I_{0.25}$ (mA cm ⁻²)
Bulk	0.60	0.355
9.3	0.60	0.351
4.9	0.60	0.348
2.0	0.48	0.231
0.81	0.53	0.304
0.62	0.59	0.436
0.47	0.53	0.107
0.16	0.45	0.098

The results showed that $I_{0.25}$, which was used to indicate the electro-catalytic activities, varied with various Pt/Au surface ratios. It increased with the increase of Pt/Au surface ratio from 0.16 to 0.62, before started to decrease as the Pt/Au surface ratio increasing until reaching about 2.0. When Pt-Au surface ratio continued to increase above 4.9, $I_{0.25}$ increased again before leveling out at the value

similar to that of Pt electrode. The same trend was also demonstrated for the shifting of onset potential. It is worth to notice that the catalytic activity of a Pt-Au catalyst to ORR maximized at Pt-Au ratio of 0.62. The phenomena could be resulted from the impacts of electrode surface structure on the adsorption energy of O₂ and other intermediate oxides in the cause of ORR.

It is well known that the ORR involves the transfer of four protons and electrons ($O_2 + 4H^+ + 4e \rightarrow 2H_2O$). In the course of ORR, several intermediates such as $-O$, $-OH$ and $-OOH$ could be involved.[9] It is generally believed that the binding energy of O₂ on Pt will increase with the increase of d-band vacancy.[6,7,13] Since the relative electronegativity value for Pt and Au are 2.2 and 2.54, respectively, the charge would transfer from Pt to Au in the Pt-Au bimetallic catalyst. This will increase of the d-band vacancy of Pt and therefore the adsorption energy of O₂ on Pt. The higher O₂ binding energy on Pt may result in a lower oxygen reduction activity of Pt.[6,13] On the other hand, the catalytic activity of the Pt-Au electrode surface is also related to the potential chemisorption of oxygen reduction reaction intermediates, such as $-OH$ which is known as the poisonous species for Pt catalyst. For a Pt-Au bimetallic catalyst the strong Au-OH bond would make the Au surface a primarily sites for the chemisorption of $-OH$ species.[7,25] Therefore the active-sites on the Pt surface are spared from the chemisorption of the poisonous species for ORR. Balancing these two effects by adjusting the Pt-Au relative surface content would elevate the Pt-Au electro-catalytic activity. In this study, when the Pt-Au surface ratio is low, the high O₂ binding energy on Pt caused by the high d-band vacancy of Pt significantly impacted on it electro-catalytic activity toward ORR. When the Pt-Au surface ratio increased, the d-band vacancy decreased, while the chemisorption on the Au surface became a dominate factor. The electro-catalytic activity of the catalyst increased according, even beyond that of a pure Pt catalyst. In this study, Pt-Au ratio of 0.62 demonstrated the maximum ORR catalytic activity. Continuous increase of Pt-Au ratio resulted in the decrease of the electro-catalytic activity, which eventually is leveled with that of a pure Pt catalyst.

Furthermore, the electrochemical stability of the Pt-Au microelectrode was also investigated. After 100 cycles of potential sweep between -0.2 to 0.8 V in an oxygen-saturated 0.1 M HClO₄ solution, the electro-catalytic activity of Pt-Au bimetallic microelectrode with surface ratio of 0.62 almost keep constant.

4. CONCLUSION

A Pt-Au bimetallic catalyst was prepared on Au microelectrode by Cu UPD followed by a spontaneous redox replacement through Pt complex ions. The tunable surface ratios of Pt/Au were achieved in a precise manner through exact Cu UPD potentials apply. The electro-catalytic performances of Pt-Au bimetallic catalyst with various surface ratios of Pt/Au toward O₂ reduction reaction were investigated. The catalytic activities of Pt-Au bimetallic microelectrode were found highly dependent with the relative surface components of Pt and Au. The optimized surface contents of Pt and Au, which demonstrated high activity and high efficiency of Pt usage, was determined as Pt/Au surface ratio of 0.62. In this Pt-Au surface configuration, the Pt-Au electrode show a positive shift of onset potential associated with the increase of kinetic current density for ORR comparing to those

detected on a pure Pt electrode. The results reported here are useful for the further design of Pt-based heterogeneous catalyst for oxygen reduction.

ACKNOWLEDGEMENTS

This work was partially supported by the Natural Science Foundation of China (11474226, 61274135, 51272200 and 51472187), National High Technology Research and Development Program ("863"Program) of China (2012AA053402) and Wuhan Science & Technology Development Program (2013011801010597).

References

1. B. C. H. Steele, A. Heinzl, *Nature* 414 (2001) 345
2. H. A. Gasteiger, N. M. Markovic, *Science* 324 (2009) 48
3. J. Zhang, K. Sasaki, E. Sutter, R. R. Adzic, *Science* 315 (2007) 220
4. Y. Tan, J. Fan, G. Chen, N. Zheng, Q. Xie, *Chem. Commun.* 47 (2011) 11624
5. P. J. Ferreira, G. J. la O', S.-H. Yang, D. Morgan, R. Makharia, S. Kocha, H. A. Gasteiger, *J. Electrochem. Soc.* 152 (2005) A2256.
6. C.-W. Liu, Y.-C. Wei, K.-W. Wang, *Journal of Colloid and Interface Science* 336 (2009) 654
7. S. S. Kumar, K. L. N. Phani, *Journal of Power Sources* 187 (2009) 19
8. N. M. Markovic, T. J. Schmidt, V. Stamenkovic, P. N. Ross, *Fuel Cells* 1 (2001) 105
9. I. E. L. Stephens, A. S. Bondarenko, U. Grønbyrg, J. Rossmeisl, I. Chorkendorff, *Energy Environ. Sci.* 5(2012) 6744
10. M. Khosravi, M. K. Amini, *Int J Hydrogen Energy* 35 (2010) 10527
11. G. Selvarani, S. S. Vinod, S. Krishnamurthy, G. V. M. Kiruthika, P. Sridhar, S. Pitchumani, *J Phys Chem C* 113 (2009) 7461
12. X. Li, J. Liu, W. He, Q. Huang, H. Yang, *Journal of Colloid and Interface Science* 344 (2010) 132
13. M. Shao, A. Peles, K. Shoemaker, M. Gummalla, P. N. Njoki, J. Luo, C.-J. Zhong, *J. Phys. Chem. Lett.* 2 (2011) 67
14. Y. Yua, Y. Hua, X. Liu, W. Deng, X. Wang, *Electrochimica Acta* 54 (2009) 3092
15. B. Lim, M. Jiang, P. H. Camargo, E. C. Cho, J. Tao, X. Lu, Y. Zhu, Y. Xia, *Science* 324 (2009) 1302
16. J. Wang, G. Yin, G. Wang, Z. Wang, Y. Gao, *Electrochem. Commun.* 10 (2008) 831
17. P. Hernandez-Fernandez, S. Rojas, P. Ocon, A.D. Frutos, J.M. Figueroa, P. Terreros, M. A. Pena, J. L. G. Fierro, *J. Power Sources* 177 (2008) 9.
18. P. Hernandez-Fernandez, S. Rojas, P. Ocon, J. L. G. Fuente, J. San-Fabian, J. Sanza, M. A. Pena, F. J. Garcia-Garcia, P. Terreros, J. L.G. Fierro, *J. Phys. Chem. C* 111 (2007) 2913.
19. J. Miomir, B. Vukmirovic, Y. Xu, M. Mavrikakis, R. R. Adzic, *Angew. Chem. Int. Ed.* 44 (2005) 2132
20. C. Wang, D. V. D. Vliet, K. L. More, N. J. Zaluzec, S. Peng, S. Sun, H. Daimon, G. Wang, J. Greeley, J. Pearson, A. P. Paulikas, G. Karapetrov, D. Strmcnik, N. M. Markovic, V. R. Stamenkovic, *Nano Lett.* 11 (2011) 919
21. J. R. C. Salgado, E. Antolini, E. R. Gonzalez, *J. Phys. Chem. B* 108 (2004) 17767
22. G. E. Ramirez-Caballero, Y. Ma, R. Callejas-Tovar, P. B. Balbuena, *Phys. Chem. Chem. Phys.* 12 (2010) 2209
23. Y.-C. Lu, H. A. Gasteiger, M. C. Parent, V. Chiloyan, S.-H. Yang, *Electrochem. Solid-State Lett.* 13 (2010) A69.
24. Y.-C. Lu, Z. Xu, H. A. Gasteiger, S. Chen, K. Hamad-Schifferli, S.-H. Yang, *J. Am. Chem. Soc.* 132 (2010) 12170.

25. J. Luo, P. N. Njoki, Y. Lin, L. Wang, C. J. Zhong, *Electrochem. Commun.* 8 (2006) 581.
26. C. Xu, R. Wang, M. Chen, Y. Zhang, Y. Ding, *Phys. Chem. Chem. Phys.* 12 (2010) 239.
27. W. Ye, H. Kou, Q. Liu, J. Yan, F. Zhou, C. Wang, *Int J Hydrogen Energy* 37 (2012) 4088
28. S. Yan, S. Zhang, *Int J Hydrogen Energy* 37 (2012) 9636
29. F. Terzia, C. Zanardia, S. Daoliob, M. Fabriziob, R. Seebera, *Electrochimica Acta* 56 (2011) 3673
30. S. R. Brankovic, J. X. Wang, R. R. Adzic, *Surf. Sci.* 474 (2001) L173.
31. M. F. Mrozek, Y. Xie, M. J. Weaver, *Anal. Chem.* 73 (2004) 5953.
32. D. Qu, C.-W. Lee, K. Uosaki. *Bull. Korean Chem. Soc.* 30 (2009) 2875.
33. Y. Wang, D. Zheng, X.-Q. Yang, D. Qu, *Energy Environ. Sci.* 4 (2011) 3697
34. D. Qu, K. Uosaki, *J. Phys. Chem. B* 110 (2006) 17570.
35. D. Qu, B.-C. Kim, C.-W. Lee, M. Ito, H. Noguchi, K. Uosaki. *J. Phys. Chem. C* 114 (2010) 497.
36. J. Clavilier, R. Faure, G. Guinet, R. Durand, *J. Electroanal. Chem.* 107 (1980) 205
37. S. Trassati, O.A. Petrii, *Pure Appl. Chem.* 63 (1991) 711.
38. H. Angerstein-Kozłowska, B.E. Conway, A. Hamelin, A, *Electrochim. Acta* 31 (1986) 1051.
39. X.R. Zhang, D.Y. Qu, L.L. Wang, C.W. Lee, *Int. J. Hydrogen Energy* 38 (2013) 5665.

© 2015 The Authors. Published by ESG (www.electrochemsci.org). This article is an open access article distributed under the terms and conditions of the Creative Commons Attribution license (<http://creativecommons.org/licenses/by/4.0/>).